

## Production of $1s$ quadrupole-orthoexciton polaritons in $\text{Cu}_2\text{O}$ by two-photon pumping

Y. Sun, G. K. L. Wong, and J. B. Ketterson

*Department of Physics and Astronomy, Northwestern University, Evanston, Illinois 60208*

(Received 22 March 2000; revised manuscript received 20 November 2000; published 13 March 2001)

We have studied the angular (at 1.8 K) and temperature dependence (from 1.8 to 70 K) of the time-integrated luminescence spectra of  $1s$  orthoexcitons from the yellow series in  $\text{Cu}_2\text{O}$  arising from resonant two-photon pumping to both the  $1s$  and  $2s$  levels. For resonant pumping to the  $1s$  level, the direct (denoted as  $X_o$ ) emission is strongly enhanced at low temperature. It is forward directed, however, with an angular width substantially larger than the divergence of the excitation beam; excitation to the  $2s$  level (which subsequently decays into a  $1s$  level) results in a more isotropic angular distribution of  $X_o$  emission. The lifetime of the  $X_o$  emission resulting from resonant excitation to the  $1s$  level at 1.8 K is  $\sim 2$  ns, shorter than the decay time of thermalized orthoexcitons. The results support the idea that resonant two-photon excitation to the  $1s$  level results primarily in a quadrupole-orthoexciton-polariton formation, whereas  $2s$  excitation does not. The behavior of the phonon-assisted luminescence is essentially independent of the mode of excitation.

DOI: 10.1103/PhysRevB.63.125323

PACS number(s): 78.55.-m

Optical excitation of a high density gas of  $1s$  (yellow) excitons in  $\text{Cu}_2\text{O}$  has been a subject of considerable interest because of the possibility of achieving excitonic Bose-Einstein condensation.<sup>1,2</sup> Exciton luminescence has been the primary tool used to probe the nature of the exciton gas. The  $1s$  orthoexciton luminescence spectrum resulting from one-photon, above-band-gap excitation has been investigated from He to room temperature. The spectrum consists of two dominant features below 150 K. One is a sharp peak due to direct electron-hole recombination emission, denoted as  $X_o$ . The other is a broader peak associated with a phonon-assisted, electric-dipole radiative transition involving  $\Gamma_{12}^-$  longitudinal optical phonons. This peak is denoted as  $X_o - \Gamma_{12}^-$ .

Recently, several studies on resonant two-photon excitation of  $1s$  excitons at low temperatures have been reported.<sup>3-7</sup> The interest was driven by the possibility that a cooler high-density exciton gas can be produced by resonant excitation. Both the  $X_o$  and  $X_o - \Gamma_{12}^-$  emissions were observed. A strongly enhanced  $X_o$  emission was explained as resonantly enhanced second harmonic generation (SHG) by Shen *et al.*<sup>3</sup> Further high-resolution two-photon spectroscopic studies of orthoexcitons near 2 K performed by Naka and Nagasawa<sup>7</sup> revealed a suppression of orthoexciton emission when the two-photon energy was within a narrow range inside the resonance, which they interpreted as a quadrupole polariton effect.

In this report, we report studies of the  $1s$  orthoexciton luminescence spectra in  $\text{Cu}_2\text{O}$  obtained by two-photon resonant pumping to the  $1s$ , as well as to the  $2s$  levels, over a wide temperature range (from 1.8 to 70 K). The  $X_o$  and  $X_o - \Gamma_{12}^-$  emissions were observed at all temperatures. The intensities of these two peaks are found to have very different temperature dependences that also depend on whether the  $1s$  or  $2s$  level was resonantly excited. At low temperature, the intensity of the  $X_o$  line was greatly enhanced when the  $1s$  level was resonantly excited. The intense emission was observed to peak strongly in the direction of the pump beam but with a divergence several times larger than that of the

pump beam. In what follows, we will argue that the enhanced forward-directed  $X_o$  emission results from the conversion of quadrupole orthoexciton-polariton waves into light at the exiting surface. We view this process as different from the resonant quadrupole second harmonic generation that was proposed<sup>3</sup> to explain the resonant enhancement of  $X_o$  emission. It is also different from the observation of Frohlich *et al.*,<sup>8</sup> who observed ‘‘quantum beats’’ in the time dependent decay of the orthoexciton luminescence as a result of the formation of coherent quadrupole-exciton polaritons at the entering surface by one-photon resonant pumping.

In our experiments, we used the frequency tripled output of a passive-active-mode-locked Nd:YAG laser to pump an optical parametric amplifier (OPA) to obtain the necessary tunable infrared radiation. The OPA output has a pulse width of 15 ps and a repetition rate of 10 Hz. The half width at half maximum (HWHM) linewidth is  $\sim 3.4$  meV. The  $\text{Cu}_2\text{O}$  samples were polished natural single crystals. The cryogenic temperatures were produced with a Janis variable-gas-flow optical cryostat and an accompanying temperature controller. The infrared laser pulses are 15 ps in length and have an energy of  $60 \mu\text{J}/\text{pulse}$ . They were focused using a 300 mm focal length lens onto the [111] surface of the sample. The spot size of the laser beam at the sample was about  $200 \mu\text{m}$ . The emitted light was collected from the opposite surface of the sample using another lens and focused onto a fiber-optic bundle, the output of which was coupled to the entrance slit of a half meter Spex SpecOne 500 M monochromator and detected using a liquid nitrogen cooled charge coupled device for measuring the integrated luminescence spectrum. A few measurements of the lifetime of the  $X_o$  emission were performed using either a photomultiplier tube (PMT) followed by an oscilloscope or a Hamamatsu streak camera to detect the signal.

When the sample was resonantly excited at 1.8 K using two-photon pumping at the  $1s$  orthoexciton energy ( $\lambda_{\text{pump}} = 1219.4 \text{ nm}$ ), we observed a bright red spot at the point on the crystal surface where the infrared (IR) beam exited. The red spot became very weak and then invisible to naked eyes

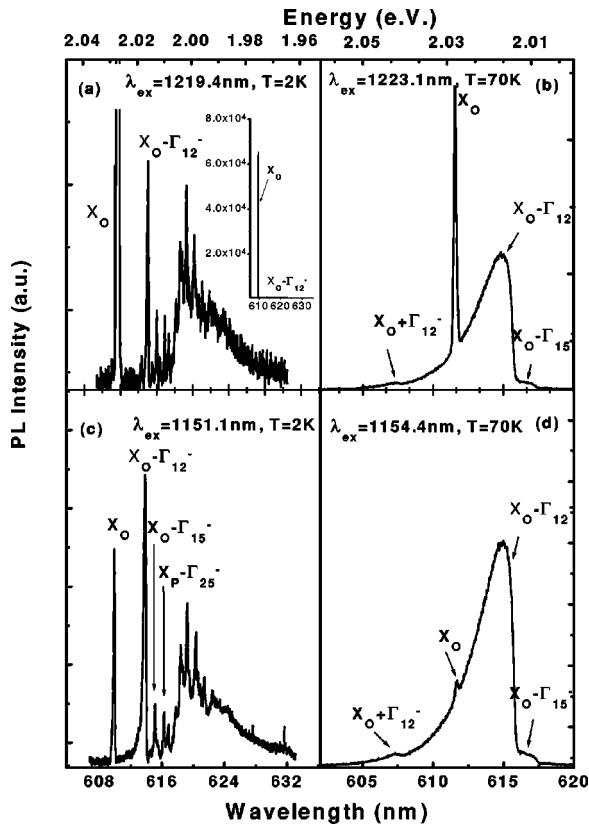


FIG. 1. Exciton photoluminescence spectra from a resonantly two-photon excited  $\text{Cu}_2\text{O}$  crystal. In all figures,  $X_0$  denotes the orthoexciton direct quadrupole emission,  $X_0-\Gamma_{12}^-$  denotes  $\Gamma_{12}^-$  optical-phonon-emission-assisted luminescence,  $X_0+\Gamma_{12}^-$  denotes  $\Gamma_{12}^-$  optical-phonon-absorption-assisted luminescence,  $X_0-\Gamma_{15}^-$  denotes  $\Gamma_{15}^-$  optical-phonon-emission-assisted luminescence, and  $X_p-\Gamma_{25}^-$  denotes  $\Gamma_{25}^-$  optical-phonon-emission-assisted paraexciton luminescence. (a) and (b) involve pumping to a  $1s$  level; (a) is measured at 2 K and the pumping wavelength is 1219.4 nm (the inset shows the full-scale spectra); (b) is measured at 70 K and the pumping wavelength is 1223.1 nm. (c) and (d) involve pumping to a  $2s$  level; (c) is measured at 2 K and the pumping wavelength is 1151.1 nm; (d) is measured at 70 K, and the pumping wavelength is 1154.4 nm.

when the IR beam was tuned off resonance. Through the polished side surfaces of the crystal, we could also see a red line traversing the sample along the path of the IR pump beam.

Figure 1(a) shows the spectrum of light emitted from the red spot. A thin  $\text{Cu}_2\text{O}$  crystal platelet ( $\sim 0.4$  mm thick) was used for these measurements so the effect of reabsorption on the spectral shape could be minimized. One sees from Fig. 1(a) that the  $X_0$  emission line has a linewidth  $< 1$  meV, much narrower than the  $\sim 3.4$  meV linewidth of the IR pumping beam, and its integrated intensity is much stronger than the  $\Gamma_{12}^-$  optical phonon-assisted recombination luminescence line, denoted as  $X_0-\Gamma_{12}^-$ . As shown in Fig. 1(b), the  $X_0$  emission line becomes much weaker at 70 K while the  $X_0-\Gamma_{12}^-$  line becomes much stronger and broader. The broadening of the  $X_0-\Gamma_{12}^-$  line is associated with an increase in

the exciton temperature. The  $\Gamma_{12}^-$  phonon-assisted spectrum is a replica of the kinetic energy distribution of the orthoexcitons. This spectrum could be well fitted with a Maxwell-Boltzmann distribution using the cryostat temperature of 70 K. This indicates that the orthoexcitons have reached thermal equilibrium with the lattice and that negligible heating of the sample occurred as a result of  $1s$  two-photon resonant excitation. Note that at 70 K, a recombination emission line associated with the absorption of  $\Gamma_{12}^-$  phonons, denoted as  $X_0+\Gamma_{12}^-$ , is also observed. Also note that two-photon resonant excitation occurs at 1219.4 nm at 2 K, whereas it is at 1223.1 nm at 70 K, in agreement with the temperature dependence of the band-gap energy. The sharp peaks superimposed on a broader band at longer wavelength are thought to be due to bound excitons on metallic impurities. The spectrum of red emission collected from a direction perpendicular to the laser beam is quite similar, except that the  $X_0$  line is much weaker.

We also measured the emission spectra under resonant two-photon excitation into the  $2s$  orthoexciton level. A strong increase in the intensities of  $X_0$  and  $X_0-\Gamma_{12}^-$  emissions was again observed under the resonant condition. No sharp emission line was observed at the  $2s$  exciton position. Figure 1(c) and Fig. 1(d) show the spectra of the  $X_0$  and  $X_0-\Gamma_{12}^-$  lines at 2 and 70 K. The general features of the spectra shown in Fig. 1(c) and Fig. 1(d) are similar to those in Fig. 1(a) and Fig. 1(b). However, for resonant pumping into the  $2s$  level, the intensity of the  $X_0$  emission is much weaker and the  $X_0-\Gamma_{12}^-$  line exhibits a high-energy tail indicating the temperature of the  $1s$  excitons was higher in this case. The above observations suggest that two-photon, resonantly excited  $2s$  excitons decay rapidly to  $1s$  excitons by some nonradiative process. The excess energy presumably goes into heating the lattice and thermalizes the  $1s$  exciton gas, giving rise to a high energy tail on the  $X_0-\Gamma_{12}^-$  line shown in Fig. 1(c).

To probe the nature of the  $X_0$  emission, we measured its angular dependence at 1.8 K under two-photon resonant excitation to the  $1s$  and  $2s$  levels. Figure 2 shows the angular distribution of the  $X_0$  emission. We see that the HWHM about the forward direction of the  $X_0$  emission under resonant excitation to  $1s$  level is about  $15^\circ$ , significantly larger than the  $5^\circ$  divergence of the IR pump beam (which was fixed by the focusing optics). In contrast the  $X_0$  emission under resonant excitation to the  $2s$  level shows a more isotropic distribution.

We have also measured the temperature dependence of  $1s$  orthoexciton luminescence from 2 to 53 K. Figure 3 shows the temperature dependence of the integrated intensity of the  $X_0$  and  $X_0-\Gamma_{12}^-$  emissions for resonant  $1s$  excitation. Between 2 and 20 K, the phonon-assisted luminescence decreases as a function of increasing temperature, reaching a minimum around 20 K and then starts to increase exponentially with temperature. The temperature dependence of the phonon-assisted emission obtained by two-photon resonant excitation to the  $2s$  level was also similar. In both cases, the temperature dependence is similar to that obtained by one-

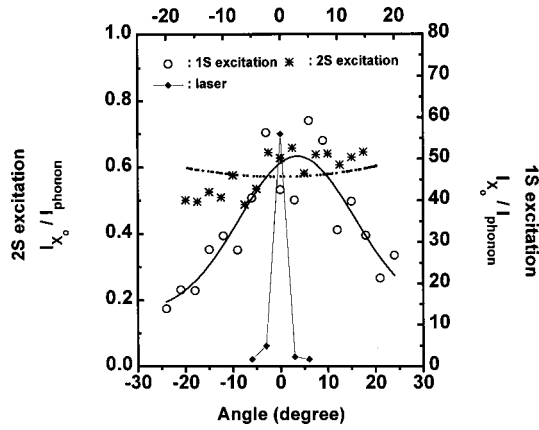


FIG. 2. Angular distribution of the ratio of the  $X_0$  emission intensity to the  $X_0 - \Gamma_{12}^-$  emission at 2 K. The hollow circles denote two-photon resonant excitation to the  $1s$  level. The stars denote two-photon excitation to the  $2s$  level. The dotted line is a theoretical fit. The solid diamonds represent the measured divergence of the laser through the optical components. We took the angular distribution of the  $X_0 - \Gamma_{12}^-$  emission intensity as a calibration in measuring the angular distribution of  $X_0$  emission intensity for two-photon excitation to both  $1s$  and  $2s$  levels.

photon above band gap excitation and can be explained using a para-ortho two-level model.<sup>9</sup>

The temperature dependence of the  $X_0$  line, however, depends on whether it was obtained using two-photon resonant excitation to the  $1s$  or  $2s$  level. Under two-photon resonant excitation to the  $1s$  level, the  $X_0$  emission intensity decreases dramatically as the temperature increases. A 100-fold increase is observed within an interval of 20 K. The temperature dependence can be well fitted with a  $T^{-3/2}$  form. For the case of  $2s$  excitation, the  $X_0$  emission intensity also increases with decreasing temperature. However, it does not show the dramatic increase at low temperatures.

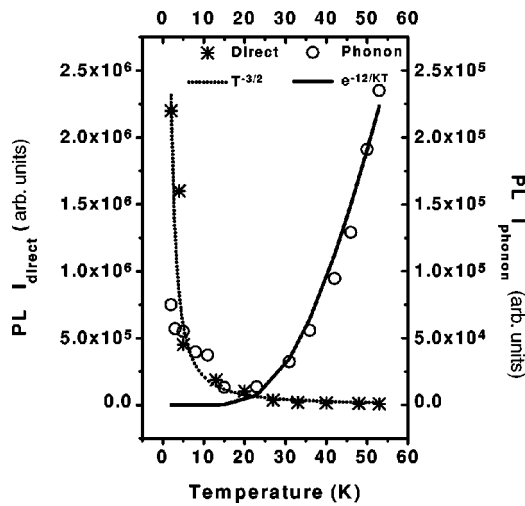


FIG. 3. Temperature dependence of the integrated intensity of  $X_0$  emission and  $X_0 - \Gamma_{12}^-$  emission arising from two-photon resonant excitation to the  $1s$  level. The stars are for the  $X_0$  emission and the hollow circles are for the  $X_0 - \Gamma_{12}^-$  emission. The dashed and solid lines are fits (see text).

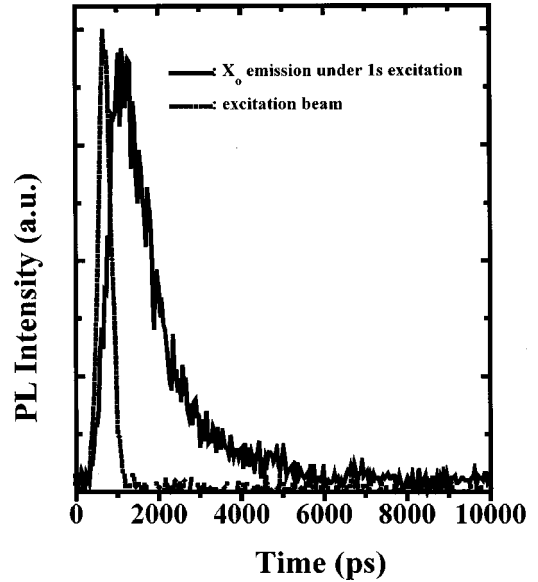


FIG. 4. Time dependence of the  $X_0$  emission arising from two-photon resonant excitation to  $1s$  level in  $\text{Cu}_2\text{O}$  at 1.8 K. The dots denote the time response of the pumping beam, while the solid line denotes the time response of the  $X_0$  emission.

The lifetime for the  $X_0$  emission under  $1s$  excitation is around 2 ns, as shown by the solid line in Fig. 4, which is much shorter than the decay time of orthoexciton photoluminescence at 1.8 K, resulting from one-photon above band-gap excitation.<sup>10</sup> The resolution of the detection system used is  $\sim 200$  ps, as shown by the response of the system to the excitation beam (dotted line). The lifetime of the  $X_0 - \Gamma_{12}^-$  and  $X_0$  emissions under  $2s$  excitation measured with a PMT followed by a fast oscilloscope, is on the order of 10 ns consistent with the reported decay time for thermalized orthoexcitons.<sup>10</sup>

We now discuss the origin of the intense and forward-directed  $X_0$  emission observed at low temperature. Shen *et al.*<sup>3</sup> attributed it to the resonantly enhanced quadrupole-second-harmonic generation. The large resonant enhancement was attributed to the narrow linewidth of the  $X_0$  line at low temperature. Our data do not support a simple SHG model. First, the divergence of the  $X_0$  emission is too large. If it were an SHG beam, it should have essentially the same divergence as the fundamental beam. We also did not observe Maker fringes when the sample was rotated. Second, conventional SHG cannot explain the temperature dependent behavior of the  $X_0$  emission and  $X_0 - \Gamma_{12}^-$  emissions as shown in Fig. 3. The linewidth of the orthoexciton  $\gamma(T)$  is proportional to  $1/(e^{\theta/T} - 1)$ ,<sup>11</sup> where  $\theta$  is equal to 220 K. When the lattice temperature  $T$  is much lower than 220 K,  $\gamma(T_2)/\gamma(T_1)$  is proportional to  $e^{(\theta/T_2 - \theta/T_1)}$ . The intensity of the  $X_0$  emission should then decrease much faster than the observed  $T^{-3/2}$  behavior. Third, the lifetime of conventional SHG should be essentially the same as the pulse width of the excitation beam. Our observation shows that the lifetime of  $X_0$  emission under  $1s$  excitation is 100 times longer than the excitation beam.

The shorter lifetime, forward-directed character, and strongly enhanced amplitude at low temperature indicate that the  $X_o$  emission obtained by two-photon 1s excitation is also different from hot luminescence, which the  $X_o$  emission from 2s excitation displays. The angular distribution of the emission from thermalized orthoexciton is governed by a selection rule resulting from the quadrupole matrix element. We find the following expression for the polarization-averaged direct decay matrix element for 1s orthoexcitons in an arbitrary direction  $\vec{k}(\theta, \phi)$

$$\bar{M} \propto \cos^2 \theta + \cos^2 2\theta + \sin^2 \theta \cos^2 2\phi + \sin^2 2\theta \sin^2 2\phi, \quad (1)$$

where  $\theta$  and  $\phi$  are Euler rotation angles with  $\theta$  and  $\phi$  measured from cube axes. Incorporating Snell's refraction law, the intensity variation of the  $X_o$  emission within  $\pm 20^\circ$  around the [111] axis is negligible, as shown by the dotted line in Fig. 2. The angular dependence of the  $X_o$  emission resulting from 2s excitation matches the theory within the scatter of our data.

Our observations are more consistent with the interpretation that  $X_o$  emission under 1s excitation arises from a resonant two-photon creation of excitons via the second-order dipole terms in the interaction Hamiltonian, which, in turn, resonantly quadrupole couple to light via polariton formation. The enhanced forward-directed  $X_o$  emission results from the conversion of coherent orthoexciton-polariton waves into light at the exiting surface. However, rather than the incoming beam decomposing into the two exciton polariton branches at the entering surface (as in the one-photon, quantum-beat experiments of Frohlich *et al.*), the IR beam acts as a source for the continuous generation of exciton polaritons as it traverses the sample.

The broadening of the angular distribution in the forward direction could be caused by small-angle, elastic-scattering of the exciton, the "mechanical" part to the polariton. Impurities and vacancies in the crystal serve as elastic scattering centers for the excitons. Assuming the distance between impurities or vacancies is, on the average, large compared to the Bohr radius of the excitons, the dominant scattering process would be associated with the strain field and the associated deformation potential and should lead to small angle deflections. Multiple scattering of excitons during the polariton propagation through the crystal could be considered as a random walk process in  $\theta$  (where  $\theta$  is now the angle between the pumping beam and observation direction), which results in a Gaussian distribution of the  $X_o$  emission intensity.

The decrease of the  $X_o$  emission with increasing temperature can be accounted for by an increase of the ortho to para down-conversion rate as a function of temperature. Theoretically, ortho to para down-conversion mechanisms were attributed to either ortho down converting to paraexciton, by

emitting an acoustic phonon, or creating two paraexcitons, by annihilating two orthoexcitons with opposite  $J_z$ .<sup>9</sup> Either process predicts an ortho-para down-conversion rate  $D \propto T^{3/2}$ , which is consistent with reported experimental results.<sup>12</sup> When the para to ortho up-conversion rate and the intrinsic decay rate of ortho and para excitons is much smaller than  $D$ , the total density of the orthoexcitons is proportional to  $1/D$  which follows from solving the steady-state rate equations.<sup>9</sup> Considering that the integrated phonon-assisted emission intensity (which samples orthoexcitons in all momentum states) is much smaller than the integrated direct emission (which only samples orthoexcitons in low momentum states), we can approximate the number of orthoexcitons involved in the polariton process as the total number of orthoexcitons at low temperature. This can approximately explain the  $T^{-3/2}$  temperature dependence of the  $X_o$  emission in our two-photon resonant case.

Qualitatively, once excitons are created by absorbing two photons at some point along the path of the fundamental beam, a polariton wave packet propagates inside the crystal with a group velocity  $v_g(\omega)$  along a direction fixed by  $\vec{k}(\omega)$ , where  $\vec{k}(\omega) = 2\vec{k}_{\text{pump}}(\omega)$ . Due to the strong dispersion for quadrupole polaritons in  $\text{Cu}_2\text{O}$ , the wave packet will spread during propagation, which results in an effective lifetime for the  $X_o$  emission. If the dephasing time is faster than the dispersion-induced pulse width, the lifetime of the  $X_o$  emission will be dominated by the former. In our case, the thickness of the sample (3.5 mm) is too long to probe the propagation time of the polariton. The dephasing time for orthoexciton polaritons is  $\tau_{\text{coh}} = 2\hbar/\Gamma = 2$  ns, where  $\Gamma = 6.5 \times 10^{-7}$  eV from the literature.<sup>8</sup> This explains the shorter lifetime of the  $X_o$  emission observed under 1s excitation.

In summary, we have observed orthoexciton luminescence over a wide temperature range arising from two-photon resonant excitation to both 1s and 2s levels. The rapid increase in the intensity of the  $X_o$  emission from 1s excitation at low temperature, its shorter lifetime relative to undressed orthoexcitons, and its forward-directed character are interpreted in terms of resonant exciton creation, which subsequently couples to light via polariton formation. It is pointed out that this is not resonant second-harmonic generation in the conventional sense. None of these features is observed for the  $X_o$  line under two-photon excitation to the 2s state, which is consistent with this explanation.

We would like to acknowledge the help of J. Ma, X. Du, and J. Y. Wu with our experiments at various stages. We would also like to thank P. Auvil, D. Snoke, J. Wolfe, and K. E. O'Hara for helpful discussions on the interpretation of our data. This work received core and facility support from the Northwestern Materials Research Center under NSF Grant No. DMR-9632472.

- <sup>1</sup>L. L. Jia and J. P. Wolfe, Phys. Rev. Lett. **71**, 1222 (1993).  
<sup>2</sup>D. W. Snoke *et al.*, Phys. Rev. B **41**, 11 171 (1990).  
<sup>3</sup>M. Y. Shen *et al.*, Phys. Rev. B **53**, 13 477 (1996).  
<sup>4</sup>T. Goto *et al.*, Phys. Rev. B **55**, 7609 (1997).  
<sup>5</sup>M. Y. Shen *et al.*, Phys. Rev. B **56**, 13 066 (1997).  
<sup>6</sup>S. Kono *et al.*, Solid State Commun. **97**, 455 (1996).  
<sup>7</sup>N. Naka and N. Nagasawa, Solid State Commun. **110**, 153 (1999).  
<sup>8</sup>D. Fröhlich *et al.*, Phys. Rev. Lett. **67**, 2343 (1991).  
<sup>9</sup>N. Caswell and P. Y. Yu, Phys. Rev. B **25**, 5519 (1982); G. M. Kavoulakis and A. Mysyrowicz, cond-mat/0001438 (unpublished).  
<sup>10</sup>A. Mysyrowicz *et al.*, Phys. Rev. Lett. **43**, 1123 (1979).  
<sup>11</sup>D. W. Snoke *et al.*, Phys. Rev. B **45**, 11 693 (1992).  
<sup>12</sup>J. S. Weiner *et al.*, Solid State Commun. **46**, 105 (1983).